International Journal of GEOMATE, June 2019, Vol.16, Issue 58, pp.41 - 47
Geotec., Const. Mat. & Env., DOI: https://doi.org/10.21660/2019.58.8128
ISSN: 2186-2982 (Print), 2186-2990 (Online), Japan

CYCLIC MECHANICAL PROPERTIES OF SANDY SOILS BY MIXING RECYCLED ASPHALT PAVEMENT MATERIAL

*Shoji Yokohama[1] and Atsuko Sato[2]

[1] Faculty of Engineering, Hokkaido University, Japan; [2] Civil Engineering Research Institute for Cold Region, PWRI, Japan

*Corresponding Author, Received: 20 Oct. 2018, Revised: 04 Dec. 2018, Accepted: 26 Dec. 2018

ABSTRACT: Reusing of recycled asphalt pavement material (RAP) as an engineering material for ground improvement is important for reducing construction or maintenance costs. Reusing of RAP for ground improvement and ground protection seems available for reduction of construction cost because there are much stocks of RAP. In this study, it is indicated that the cyclic mechanical properties of the sandy soil improved by mixing RAP. In order to obtain the fundamental results for the effect of mixing RAP on the improvement of cyclic behavior, the series of cyclic undrained triaxial tests were conducted. From the test results, it is shown that the cyclic strength of sandy soil - RAP mixture was greater than the cyclic strength without RAP case. It is also shown that the accumulation speed of excess pore water pressure at sandy soil - RAP mixture is slower than that without RAP mixing. In addition, the mechanism for cyclic mechanical properties of sandy soil - RAP mixture is also suggested.

Keywords: Recycled asphalt pavement material, Cyclic behavior, Sandy soil, Volcanic Soil

1. INTRODUCTION

Recycling of industrial waste materials is actively promoted in civil engineering work. In order to progress using recycled asphalt material as a construction material, many research for the mechanical properties of recycled asphalt pavement or recycled asphalt shingle has conducted and good performance of recycled asphalt pavement has pointed out by [1-6]. When the road pavement is restored, recycled asphalt pavement gravel material and newly gravel materials are mixed to properly make effective use of construction materials. Therefore, it is difficult to secure the storage space for asphalt waste material because the amount of waste material has been increased.

On the other hand, it is necessary to realize constructing the flexible earth structure or improving seismic mechanical properties of ground for reducing the ground disasters. In this study, the fundamental data for mechanical properties of sandy soil mixed with the recycled asphalt pavement material (RAP) are obtained from the series of laboratory tests. The series of cyclic undrained triaxial tests are conducted. First, the basic data for the cyclic mechanical properties of RAP - fine sand mixture are investigated. Next, the mechanical properties of a mixture of RAP and volcanic coarse-grained soil are also discussed. From these results, it is shown that the cyclic undrained strength of the mixture of RAP - fine sand or volcanic coarse-grained soil is higher than those without RAP mixing. In addition, to investigate the influence of specimen temperature on the cyclic strength, the cyclic undrained triaxial tests are conducted at a temperature of 50 ºC. It is also clarified that the specimen temperature and the magnitude of the effective confining pressure affect the cyclic mechanical characteristics of the mixture of RAP - volcanic coarse-grained soil.

2. FIELD APPLICATION

One example of ground protection works utilizing the recycled asphalt pavement material is introduced in this paper. Fig.1 shows one situation of the ground protection by laying RAP at the site in Hokkaido, Japan. In order to prevent muddy ground due to the rainfall or snow melting, the protection work was performed on June 2009. RAP material was laid on the ground surface with a thickness of 100mm. The persons and vehicles for forestry work can easily pass on the protected ground surface. Even though water is provided by heavy rain or snow melting on the ground, remarkable erosion has not seen for about 9 years. The temperature of the ground surface at the site is shown in Fig.2. The ground temperature is monitored since April 2016. As can be seen from Fig.2, the temperature reached about 50 °C in the summer and about -20 °C in the winter. The result indicates that the temperature change behavior of RAP is sensitive.

The soil hardness on the protected ground surface is shown in Fig.3 and Table.1. The soil hardness is measured by the handy soil penetrometer shown in Fig.4. When the soil

Fig.1 Ground protection by RAP

Table 1 List of measurement data for soil hardness

Mesurement date	Elapsed time (day)	Soil hardness (mm)		
		Average value	Maximun value	Minimun value
27, APR, 2016	0	25.9	30.5	20.0
18, MAY, 2016	21	31.7	33.5	29.5
22, JUN, 2016	56	31.0	34.0	28.5
27, JUL, 2016	91	30.0	27.5	34.0
26, AUG, 2016	121	30.1	35.0	26.0
7, OCT, 2016	163	30.1	33.5	27.5
11, NOV, 2016	198	35.8	40.0	31.0
23, MAR, 2017	330	24.0	33.0	16.5

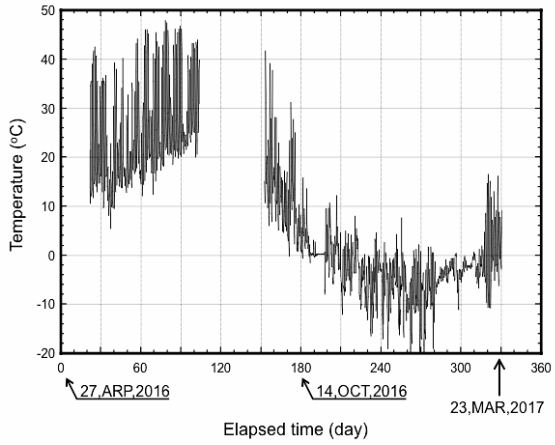

Fig.2 Temperature on ground protected by RAP

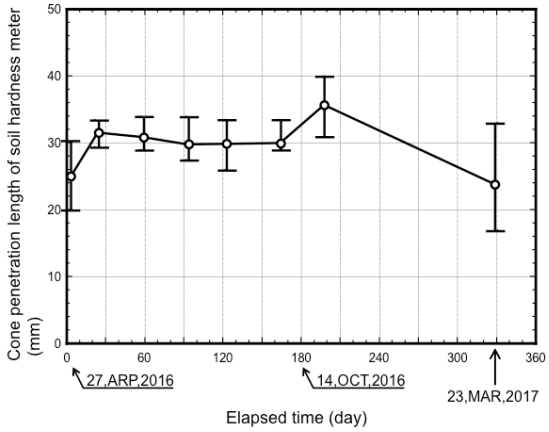

Fig.3 Soil hardness on Protected ground

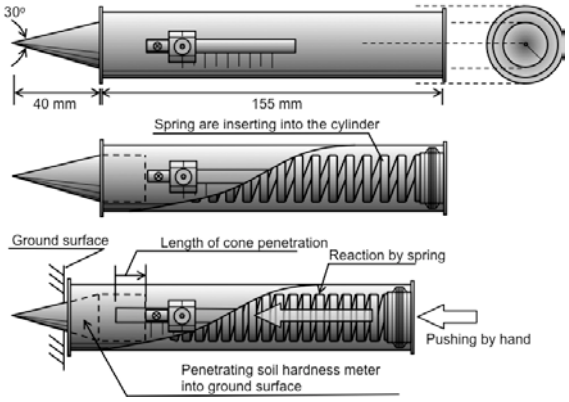

Fig.4 Soil hardness meter (handy type)

hardness is measured, the cone of handy soil penetrometer is inserted in the protected ground. The penetration length of the cone of penetrometer is recorded as the soil hardness value. 10 data of soil hardness at the protected slope surface were measured at one testing. The average of 10 data is evaluated as the soil hardness value in this study. From Fig.3, it is recognized the soil hardness is slightly lower in the spring season (April 27, 2016, and March 23, 2017) than the other periods. The soil hardness did not decrease even under high-temperature condition such as the summer season. From the obtained data, it is found that the protected ground by RAP can keep its stable state throughout the year.

3. TESTING MATERIALS

In this study, recycled asphalt pavement material (RAP) and some sandy soils are prepared for testing materials. RAP is the recycled aggregate produced from deteriorated asphalt pavement. RAP is sampled in Sapporo city on August 2014. Fig.5 shows the appearance of RAP particles. The black object on the surface of RAP particle seems as asphalt binder. Toyoura sand (T sand) and one of the volcanic coarse-grained soil (Shikotsu pumice flow deposits, Spfl) are also adapted for the testing materials.

Fig.6 shows the external appearance of Spfl particles. Many volcanic soils including Spfl have unique mechanical characteristics such as the many cavities in the soil particles and particles breakage behavior [8, 9]. In order to indicate the effects of RAP mixing on the cyclic mechanical behavior of sandy soils, the cyclic undrained triaxial tests are conducted by using RAP-T sand mixture (As-T sand) and RAP-Spfl mixture (As-Spfl). The grain size distribution and the list of

Fig.5 RAP particles

Fig.6 Spfl particles

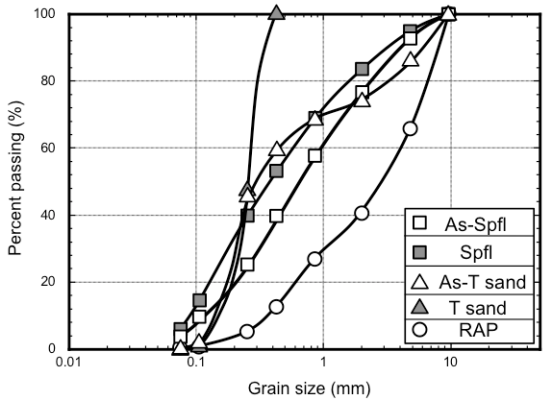

Fig.7 Grain size distribution

index properties of the test samples are shown in Fig.7 and Table.2, respectively. For As-T sand and As-Spfl, the mixing ratio of RAP, M_{AS}/M_s is 50%. M_{AS} and M_s are the dry mass of RAP and the dry total mass of specimen, respectively.

4. TEST PROCEDURE

The specimens for cyclic undrained triaxial tests are prepared by air pluviation of soil particles into the mold. The diameter and height of the specimen are 70 and 150 mm, respectively. Carbon dioxide is percolated and de-aired water is slowly permeated from the bottom to the top of the specimen. Thereafter, backpressure of 200 kPa is

Table 2 Index properties of testing materials

	ρ_s (Mg/m^3)	ρ_{dmax} (Mg/m^3)	ρ_{dmin} (Mg/m^3)	F_c (%)	M_{As}/M_s (%)
Recycled asphalt pavement material (RAP)	2.366	1.607	1.412	---	100
Volcanic soil (Spfl)	2.453	1.005	0.778	6.15	0
RAP and Spfl mixture (As-Spfl)	2.466	1.306	1.038	3.11	50
Toyoura sand (T sand)	2.649	1.636	1.344	---	0
RAP and T sand mixture (As-T sand)	2.516	1.805	1.462	---	50

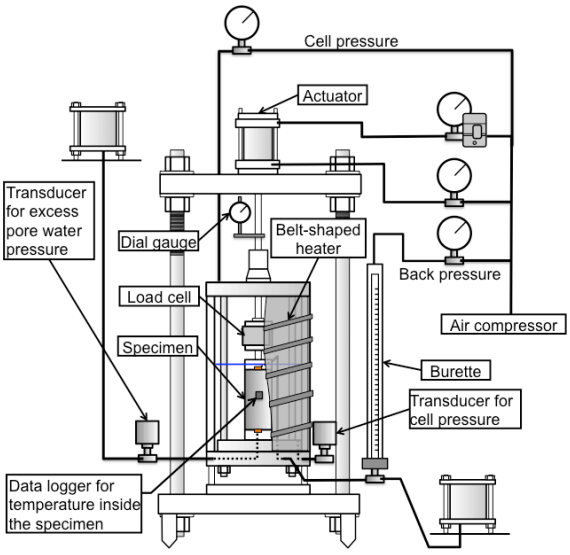

Fig.8 Apparatus for cyclic triaxial test

applied into the specimen. Application of backpressure is carried out until the pore pressure coefficient B-value reaches 0.95 or above. The isotropic consolidation is conducted under the confining pressure σ'_c of 50 and 100 kPa. The isotropic consolidation is continued until the volumetric strain rate is less than 1.0×10^{-4} %/min. After isotropic consolidation, the cyclic deviator stress is applied to the specimen with 0.1 Hz in frequency.

In order to investigate the effects of specimen temperature on the cyclic mechanical properties, the series of cyclic undrained triaxial tests are also conducted under a high-temperature condition. Fig.8 illustrates the test apparatus under a high-temperature condition. Hot water is poured into the triaxial cell. The specimen temperature is kept by winding the belt-shaped heater round the triaxial cell. Furthermore, the heat-insulation sheet is also wrapped around the triaxial cell. The thermo-sensor shown in Fig.9 is installed into the center of the specimen. The example data for the specimen temperature recorded by the thermo-sensor is

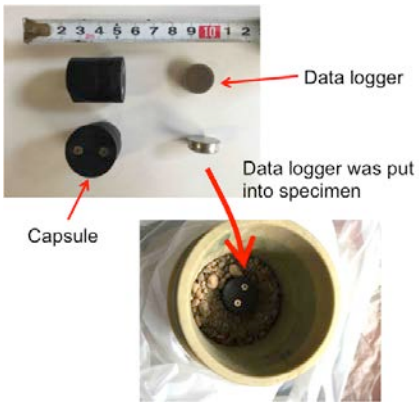

Fig.9 Temperature logger in the specimen

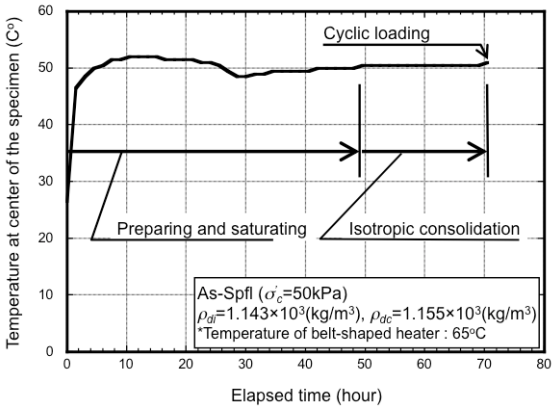

Fig.10 Specimen temperature (As-Spfl)

shown in Fig.10. The specimen is prepared by As-Spfl at the dry density ρ_{dc}=1.155Mg/m^3. The temperature of the belt-shaped heater is set to 65 °C. It can be seen the specimen temperature is kept about 50 °C from start to end. In this study, the specimen temperature is set to 50 °C by this heating method.

5. RESULTS AND DISCUSSIONS

5.1 Cyclic Behavior of As-T Sand

Firstly, the cyclic mechanical behavior of RAP and T sand mixture is mentioned. Fig.11 shows the relationship between cyclic stress ratio $\sigma_d/2\sigma'_c$ and the number of loading cycles N_c to cause the double amplitude of axial strain *DA* of 5 % for As-T sand, and T sand specimens. The list of test results is shown in Table.3. In order to get the reliable results, the cyclic tests were carried out at least 4 or 5 times per one of the $\sigma_d/2\sigma'_c$ - N_c curve. In order to show the mechanical trend of RAP specimen, the $\sigma_d/2\sigma'_c$ - N_c curve is drawn by only 3 data is also plotted in Fig.11. σ_d and σ'_c are the amplitude of cyclic deviator stress and effective confining pressure, respectively. These results are

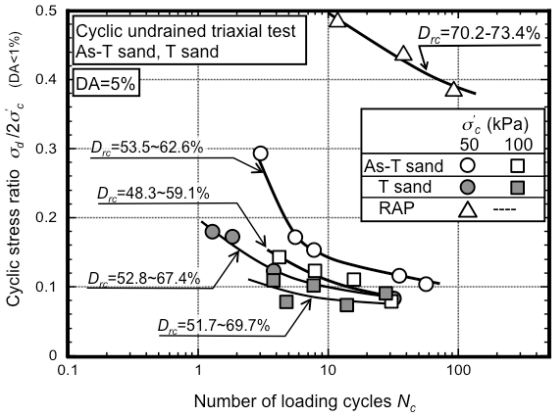

Fig.11 Cyclic strength (T sand, As-T sand)

Table 3 List of test result for As-T sand and T sand

	M_{As}/M_s (%)	σ'_c (kPa)	ρ_{dc} (Mg/m^3)	D_{rc} (%)	$\sigma_d/(2\sigma'_c)$	N_c (DA=5%)	N_c (DA=10%)
As-T sand	50	50	1.627	53.5	0.10	56.8	58.8
			1.641	57.3	0.15	7.8	8.8
			1.649	59.8	0.12	35.2	36.9
			1.645	58.4	0.17	5.6	8.0
			1.645	58.7	0.29	3.0	5.0
		100	1.610	48.3	0.10	30.7	32.0
			1.633	55.0	0.10	16.3	18.4
			1.647	59.1	0.13	15.8	17.7
			1.646	58.9	0.15	7.9	9.4
			1.611	48.6	0.17	4.2	5.4
T sand	0	50	1.492	55.6	0.1	32.0	32.8
			1.528	67.4	0.17	1.8	2.9
			1.514	62.8	0.12	3.8	4.7
			1.484	52.8	0.18	1.3	1.7
		100	1.535	69.7	0.13	3.80	5.01
			1.516	63.5	0.12	7.75	8.85
			1.481	51.7	0.10	4.77	5.10
			1.485	53.2	0.11	27.74	28.01
			1.502	58.9	0.09	14.05	14.80
RAP	100	50	1.550	73.4	0.38	92.75	—
			1.544	70.2	0.44	37.93	—
			1.547	71.8	0.48	11.85	—

obtained at σ'_c = 50 and 100 kPa under room temperature conditions. It is seen that $\sigma_d/2\sigma'_c$ at As-T sand is higher than that of T sand. The value of $\sigma_d/2\sigma'_c$ for RAP is highest of all. However the effect of the difference of the grain size distribution between RAP and As-T sand cannot be ignored, it is recognized that the cyclic strength is improved by mixing RAP with T sand particles.

The excess pore water pressure ratio $\Delta u/\sigma'_c$ and N_c relations at σ'_c = 50 and 100 kPa are shown in Figs.12 (a) and (b). It can be seen that N_c until reaching $\Delta u/\sigma'_c$ =0.95 for As-T sand specimen is larger than that at T sand specimen. In addition, the accumulation speed of the excess pore water pressure seems to slow down due to mixing RAP. Such tendency is remarkable at σ'_c = 50 kPa than the case at σ'_c = 100 kPa. At σ'_c = 100 kPa case, the difference of $\Delta u/\sigma'_c$ between As-T sand and T

sand is very small. Despite the similarity of excess pore water pressure behavior, the difference in cyclic strength between As-T sand and T sand is recognized in Fig.11. Contacting between RAP and T sand particles may cause the change in cyclic deformation characteristic.

In order to observe the deformation behavior of specimens after cyclic loading, Figs.13 (a), (b) and (c) display the photographs of the specimen for As-T sand, T sand and RAP, respectively. At As-T sand specimen shown in Fig.13 (a), the specimen keeps its cylindrical shape after cyclic loading. The adhesive bonding [10] may lead to this behavior. From Fig.13 (b), it is seen that T sand specimen failed to maintain its cylindrical shape and flow deformation is observed after the cyclic loading. From Fig.13 (c), the tensile behavior of RAP specimen is seen after cyclic loading. The pattern of such deformation behavior seems different from the As-T sand and T sand specimens.

5.2 Cyclic Behavior of As-Spfl

The cyclic strength for As-Spfl and Spfl specimens are also verified. The relationships between $\sigma_d/2\sigma'_c$ and N_c to cause the DA value of 5 % are shown in Figs.14 (a) and (b). The list of test results is also shown in Table.4. For each testing case, the cyclic tests are carried out at least 4 times. In these figures, the test results at the specimen temperature of 50 ºC at As-Spfl specimen are also included. From these figures, it is found that $\sigma_d/2\sigma'_c$ of As-Spfl is higher than that of Spfl. It is also found that the difference of specimen temperature causes the difference of cyclic stress ratio $\sigma_d/2\sigma'_c$ for As-Spfl. Based on these results, it is revealed that mixing of RAP lead improving the cyclic mechanical properties of volcanic soil and the confining pressure and specimen temperature influenced the cyclic strength.

Figs.15 (a) and (b) show the relationships between $\Delta u/\sigma'_c$ and N_c for As-Spfl and Spfl specimens at σ'_c = 50 and 100 kPa, respectively. In these figures, the relative density after isotropic consolidation D_{rc} is 47 to 62 %, and the cyclic stress ratio is about 0.22. It is found that the $\Delta u/\sigma'_c$ is accumulated rapidly for Spfl specimen from Fig.15 (a). On the other hand, there is no noticeable difference of $\Delta u/\sigma'_c$ between As-Spfl and Spfl specimens in Fig.15 (b). These results denote that the mixing of RAP makes the liquefaction resistance higher.

5.3 Mechanism for Cyclic Behavior of Sandy Soil – RAP Mixture

The mechanism of cyclic deformation for the sandy soil - RAP mixture is expressed in Fig.16.

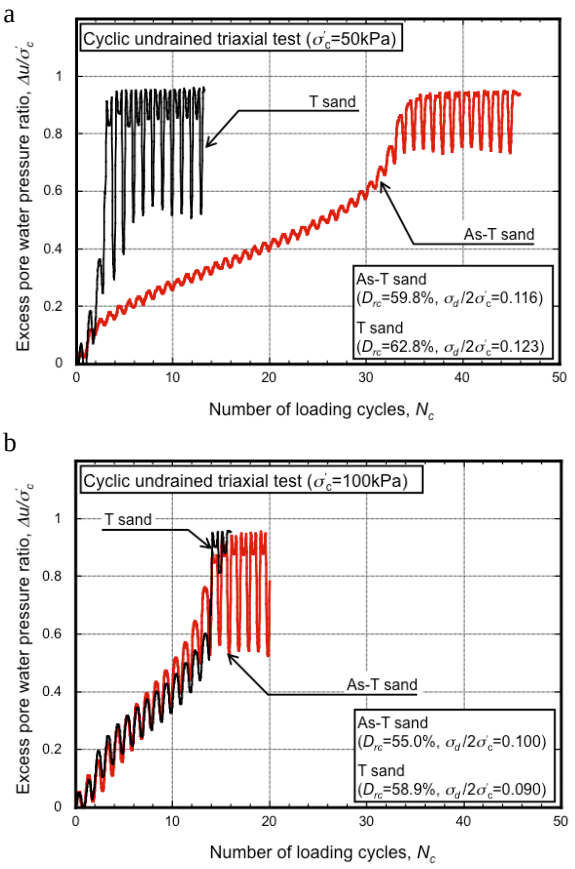

Fig.12 Excess pore water pressure ratio (T sand, As-T sand) : (a) σ'_c=50kPa, (b) σ'_c=100kPa

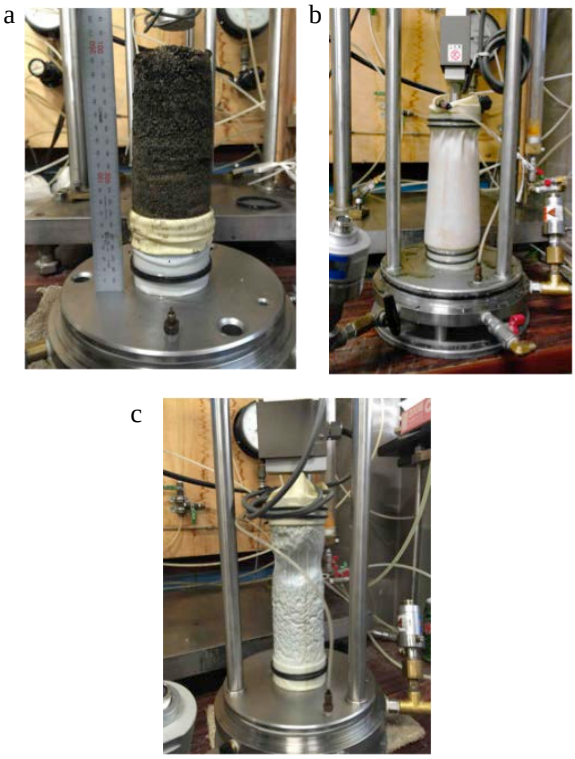

Fig.13 Appearance of specimen after cyclic loading : (a) As-T sand, (b)T sand, (c)RAP

a

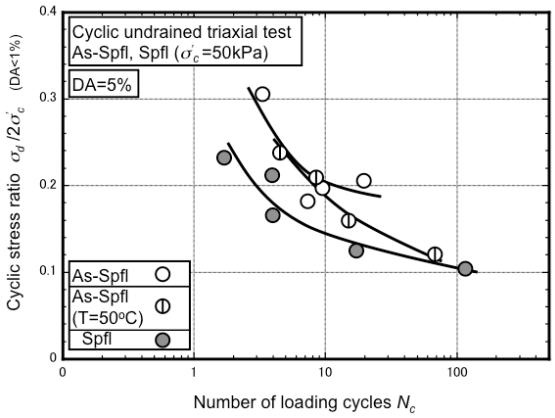

b

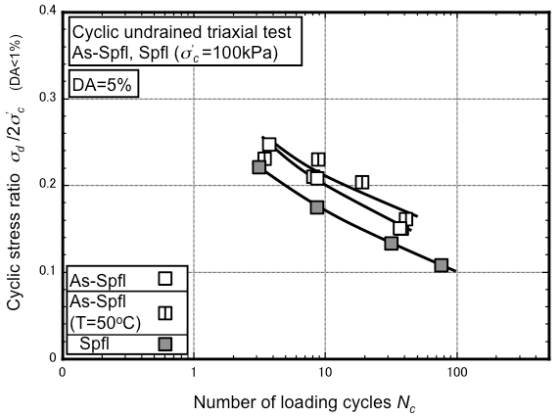

Fig.14 Cyclic strength (As-Spfl, Spfl) : (a) σ'_c=50kPa, (b) σ'_c=100kPa

Table 4 List of test results for As-Spfl and Spfl

	M_{fc}/M_f (%)	σ'_c (kPa)	ρ_{wc} (Mg/m³)	D_{rc} (%)	$\sigma_d/(2\sigma'_c)$	N_c (DA=5%)	N_c (DA=10%)
As-Spfl, 20°C	50	50	1.162	52.0	0.31	3.3	5.5
			1.146	46.1	0.18	7.3	10.5
			1.123	37.0	0.21	19.5	24.7
		100	1.183	59.8	0.20	9.4	12.6
			1.168	54.1	0.21	9.1	13.7
			1.186	60.9	0.21	8.6	11.7
			1.198	65.0	0.15	36.9	41.7
			1.167	54.0	0.21	8.1	11.6
			1.134	41.3	0.25	3.7	7.0
As-Spfl, 50°C	50	50	1.141	43.8	0.21	8.5	13.7
			1.155	49.2	0.16	14.9	22.6
			1.155	49.3	0.12	67.6	–
			1.15	47.6	0.24	4.5	7.7
		100	1.157	50	0.15	32.6	37.8
			1.162	51.9	0.16	31.8	40.6
			1.150	47.4	0.20	13.7	18.9
			1.142	44.4	0.23	1.7	3.4
			1.142	44.4	0.23	5.4	8.8
Spfl 20°C	0	50	0.894	57.4	0.17	4.0	5.0
			0.893	57.2	0.12	17.0	18.9
			0.877	49.8	0.23	1.7	2.7
			0.878	50.5	0.21	3.9	5.5
		100	0.883	52.8	0.10	115.3	121.0
			0.885	53.5	0.11	76.2	78.8
			0.885	53.4	0.13	31.8	34.7
			0.906	62.4	0.22	3.1	5.2
			0.898	59.0	0.17	8.6	11.5

a

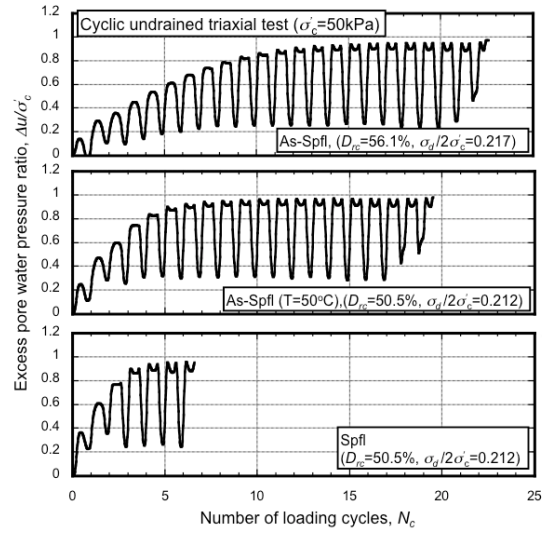

b

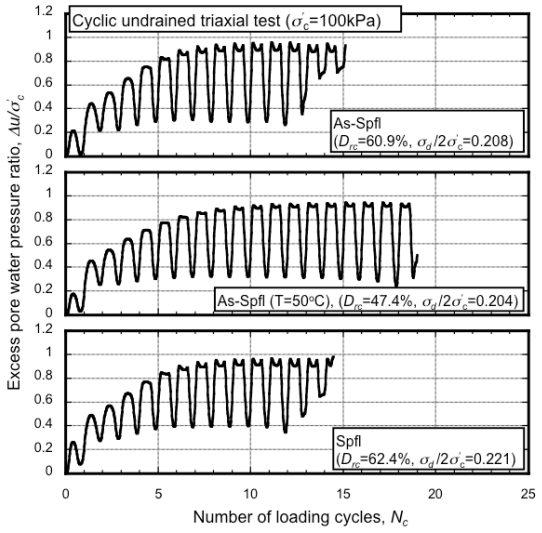

Fig.15 Excess pore water pressure ratio (As-Spfl, Spfl) : (a) σ'_c=50kPa, (b) σ'_c=100kPa

Fig.16 illustrates the *p'-q* relationships for the sandy soil. Where, *p'* and *q* are effective mean principal stress and deviator stress, respectively. For sandy soil, the effective stress decreased quickly due to the accumulation of the excess pore water pressure by cyclic undrained loading. The sandy soil behaves the cyclic mobility when the effective stress reaches to zero. On the other hand,

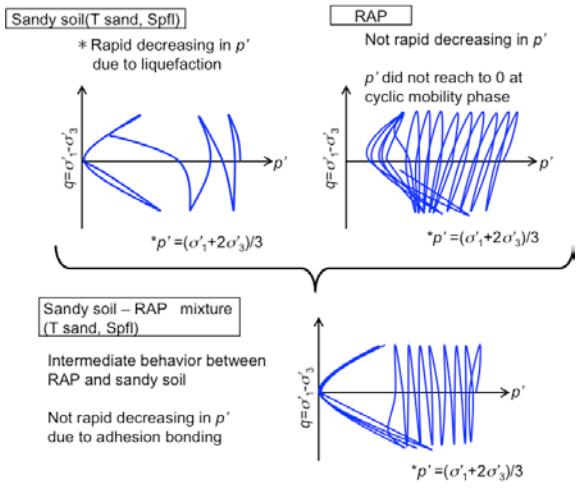

Fig.16 Mechanism of cyclic behavior for sandy soil – RAP mixture

the effective stress is not decreasing so much at RAP specimen. Additionally, the effective stress does not reach zero due to cyclic loading. Finally, the sandy soil – RAP mixture shows the intermediate behavior between sandy soil and RAP specimen. Many numbers of loading cycles are required until the effective stress reaches zero. The effective stress decreases slowly due to cyclic loading. One of the reasons for delaying effective stress reduction seems the bonding effect between RAP and sandy soil particles.

6. SUMMARY AND CONCLUSIONS

Improvement of cyclic undrained mechanical properties for sandy soils by RAP mixing is denoted in this study. It is indicated that the cyclic strength of As-T sand and As-Spfl is about 1.3 times to T sand and Spfl, respectively. For As-T sand specimen, the shape-keeping effect is recognized after the cyclic loading as like as adhesion bonding effect shown in the sandy soil.

The effect of specimen temperature on the cyclic undrained strength for As-Spfl specimen is also discussed. At the confining pressure in 50 kPa, the cyclic strength at 50 ºC condition is smaller than that at room temperature condition. On the other hand, at the confining pressure of 100 kPa, the cyclic strength at 50 ºC condition is slightly higher than that at room temperature. These experimental results show the cyclic strength for As-Spfl is affected by both confining pressure and specimen temperature.

Accumulation of excess pore water pressure ratio for As-T sand and As-Spfl specimens are slower than T sand and Spfl specimens. Such slow accumulation of excess pore water pressure may be led by interaction between RAP and sandy soil particles.

7. ACKNOWLEDGMENTS

I received generous support of field investigation for ground protection from Mr. Juichi Hatakeyama. This study was supported by JSPS KAKENHI Grant Number JP18K04341.

8. REFERENCES

[1] Viyanant, C., Rathje, E. M., and Rauch, A.F., Creep of compacted recycled asphalt pavement, Canadian Geotechnical Journal. 44, 2007, pp.687-697.

[2] Li, L., Benson, C.H., Edil. T.B., and Hatipoglu, B., Sustainable construction case history: Fly ash stabilization of recycled asphalt pavement material. Geotechnical and Geological Engineering. 26, 2008, pp.177–187.

[3] Shu, X., Huang, B., and Vukosavljevic, D., Laboratory evaluation of fatigue characteristics of recycled asphalt mixture, Construction and Building Materials. 22, 2008, pp.1323-1330.

[4] Wen, H., Warner, J., Edil, T., and Wang, G., Laboratory comparison of crushed aggregate and recycled pavement material with and without high carbon fly ash. Geotechnical and Geological Engineering. 28, 2010, pp.405-411.

[5] Soleimanbeigi, A., Edil, T.B., and Benson, C., Evaluation of fly ash stabilization of recycled asphalt shingles for use in structural fills. Journal of Materials in Civil Engineering, ACSE, 25(1), 2013, pp.94-104.

[6] Soleimanbeigi, A., Edil, T.B., and Benson, C.H., Creep response of recycled asphalt shingles. Can. Geotech. J., 51, 2014, pp.103-114.

[7] Soleimanbeigi, A., Edil, T.B., and Benson, C., Evaluation of fly ash stabilization of recycled asphalt shingles for use in structural fills. Journal of Materials in Civil Engineering, ACSE, 25(1), 2013, pp.94-104.

[8] Miura. S., Yagi. K., and Asonuma. T., Deformation-strength evaluation of crushable volcanic soils by laboratory and in-situ testing. Soils and Foundations. 43(4), 2003, pp.47-57.

[9] Matsumura, S., Miura, S., Yokohama, S., and Kawamura, S., Cyclic deformation-strength evaluation of compacted volcanic soil subjected to freeze-thaw sequence. Soils and Foundations. 55(1), 2015, pp.86-98.

[10] Lee, K.L., Adhesion bonds in sands at high pressure, Journal of the Geotechnical Engineering Division, Proceedings of the ASCE, 103, GT8, 1977, pp.908-913.